

The Effect of Low Concentrations Nb and C on the Structure and High-Temperature Strength of Fe₃Al Aluminide



PETR KRATOCHVÍL, MARTIN ŠVEC, and VĚRA VODIČKOVÁ

The Fe₃Al iron aluminide alloyed by low concentrations of Nb and C (c_{Nb} , c_{C}) is studied. The influence of the $c_{\text{Nb}}/c_{\text{C}}$ ratio on the structure and high-temperature yield strength of iron aluminide was investigated. The structure and phase composition were studied by scanning electron microscope equipped with EDS and EBSD. The strengthening mechanisms are detected as strengthening by incoherent precipitates of NbC and as a solid solution hardening by Nb atoms.

DOI: 10.1007/s11661-017-4174-y

© The Minerals, Metals & Materials Society and ASM International 2017

I. INTRODUCTION

IRON aluminide-based alloys are ideal candidates for the development of new structural materials with improved performance in petrochemical, power-generation, and aeronautical applications.^[1,2] They have excellent resistance to oxidation and sulfidation. Their density is about two thirds of the steel density. Moreover, they have high electrical resistance. The input raw materials are relatively cheap due to their occurrence in the earth's crust. The main drawbacks of these alloys are a bad workability at room temperature and low high-temperature (HT) strength. The low-temperature plasticity can be improved by the off-stoichiometric compositions, ternary additives (chromium, molybdenum, and manganese), and grain-refining agents (TiB₂ and Ce). Improvements in the creep resistance and strength are given by solid solution hardening and/or precipitation hardening.

The HT mechanical properties of Fe₃Al-type alloys can be enhanced using a variety of methods (for an overview see *e.g.*, References 3 and 4). Especially, effective method is the addition of elements with a low solubility in the Fe₃Al-matrix.

Niobium has a potential for both solid solution hardening and precipitation strengthening of Fe₃Al aluminide. The beneficial effect of niobium addition on

e.g., creep resistance was first reported by McKamey and Maziasz.^[5-7] The results obtained in a complex alloy FA-180 containing 28Al, 5Nb, 0.8Mo, 0.025Zr, 0.05C, 0.005B (atomic percent is given throughout) are summarized in Reference 7. The annealing for 1 hour at 1423 K (1150 °C) followed by quenching was successfully used to obtain the longest creep rupture live-time and the slowest minimum creep rate in creep tests at 866 K (593 °C). The microstructural analysis revealed that the strengthening was due to a dispersion of fine Nb- and Zr-rich carbides in the matrix and along grain boundaries.

Extensive study of niobium additions to Fe₃Al-based alloys was reported by Morris *et al.*^[8-11] The improvement of mechanical properties at elevated temperatures was disappointingly small. On the other hand, it was shown by Yu and Sun^[12] that addition of 0.5 at. pct Nb to Fe-28Al-4Cr (at. pct) alloy increased creep rupture live-time by one order of magnitude. A similar beneficial effect on high-temperature strength and creep resistance was observed for a small (0.83 at. pct) addition of niobium to Fe-16Al-0.43C (at. pct) alloy.^[13] On the contrary, the same author reported that addition of niobium up to 1.1 at. pct to Fe-19Al-3.65C (at. pct) alloy “did not exhibit any significant improvement in either creep life or minimum creep rate.”^[14]

The influence of 9.5 at. pct Nb on Fe-26Al (at. pct) alloy was studied in both directionally solidified and as-cast states. Creep properties of directionally solidified alloy were comparable to those of P92 steel.^[15] The structure^[16] and mechanical properties^[17] of Fe-26Al (at. pct) based alloys with alloying additions of Nb (2 and 4 at. pct) and C (1 at. pct) were also investigated. The presence of NbC carbide and Laves phase (Fe, Al)₂Nb was identified both in the as-cast and annealed alloys.

It is the purpose of the present paper to study the structure and HT mechanical properties of Fe₃Al-based

PETR KRATOCHVÍL is with the Faculty of Mathematics and Physics, Charles University of Prague, Ke Karlovu 5, 121 16 Prag, Czech Republic. MARTIN ŠVEC and VĚRA VODIČKOVÁ are with the Department of Material Science, Faculty of Engineering, Technical University of Liberec, Studentská 1402/2, 46117 Liberec, Czech Republic. Contact e-mail: martin.svec@tul.cz

Manuscript submitted February 24, 2017.

Article published online June 20, 2017

alloy with niobium and carbon additions. Since the contamination by carbon is inevitable in industrial production of this type of alloys, the alloys with different content of carbon were examined. The HT strength is related to the presence of particles of phases in the investigated alloys.

II. EXPERIMENTAL

Two alloys—FA0.2C ($c_{\text{Nb}}/c_{\text{C}} = 6$) and FA0.8C ($c_{\text{Nb}}/c_{\text{C}} = 1.38$) were investigated. Their chemical compositions were determined by the wet analysis and are given in Table I. The samples were prepared using vacuum induction melting and casting and after that they were hot-rolled at 1473 K (1200 °C) with total reduction 50 pct in several steps with 15 pct thickness reduction for each pass. The hot-rolled samples were used for structure investigation and compression tests.

The surface of alloys for the study of microstructure and phase identification was prepared by standard metallographic methods followed by mechanical-chemical polishing using OP-S suspension (Struers). Scanning electron microscope (SEM) Zeiss Ultra Plus equipped with an Oxford 20 mm² detector for energy-dispersive X-ray analysis (EDX) was used for structure investigation. Phase identification and grain sizes (step size 3 μm, HV 20 kV) were determined by electron backscatter diffraction (EBSD) using Oxford NodlysNano detector. The Nb amount dissolved in the matrix was determined by EDX. The volume fractions of the observed phases were evaluated by means of image analysis NIS—Elements of SEM—images taken in backscattered electrons (BSE) contrast.

The samples (prisms 6 × 6 × 8 mm) for HT compression tests were prepared by spark machining. The compression yield stress $\sigma_{0.2}$ was measured using INSTRON 1186 at temperature 473 K, 673 K, 873 K, and 1073 K (200 °C, 400 °C, 600 °C, 700 °C, and 800 °C) with the initial strain rate $1.5 \times 10^{-4} \text{ s}^{-1}$.

III. EXPERIMENTAL RESULTS AND DISCUSSION

A. Structure of FA0.2C Alloy

The grains of alloy FA0.2C are coarse and of hundreds of micrometers in size (Figure 1). A few oval-shaped (size 1 to 5 μm) precipitates were observed inside the grains (Figure 2) and they were identified by EBSD as NbC. The volume fraction (f_v) of NbC precipitates is 0.6 pct. The rest of Nb (0.9 at. pct) measured by EDX is dissolved in the matrix.

B. Structure of FA0.8C Alloy

The precipitates in alloy FA0.8C are also NbC carbides. They form an eutectic configuration (Figure 3) with the matrix. The individual NbC precipitates are circular or oval-shaped with dimensions of several micrometers. The grains are clearly visible using EBSD (Figure 4). They are very coarse with dimensions ranging from hundreds of micrometers to 1 to 2 mm. The amount of niobium and carbon is similar in FA0.8C—so $c_{\text{Nb}}/c_{\text{C}}$ ratio is 1.4. Almost all Nb is forming NbC ($f_v = 1.7$ pct) and only very few Nb atoms are left for the solid solution hardening of matrix (see also data in Table II).

C. The Yield Strength at HT

The values of yield strength $\sigma_{0.2}$ are decreasing with the increasing temperature for both tested alloys as well as for alloy Fe-26Al-2Nb-1C^[17] (see Figure 5). Table II summarizes the reasons of the complex effect of low alloying of Fe₃Al aluminide by Nb and C on $\sigma_{0.2}$ in the temperature range 473 K to 1073 K (200 °C to 800 °C). Obviously, $\sigma_{0.2}$ is determined both by precipitation hardening (described by f_v) and by solid solution hardening due to the amount of niobium left in the matrix. Moreover, the geometry of carbides distribution and their shape is important. The result is a complex dependence of $\sigma_{0.2}$ on temperature for all three alloys presented in Figure 5. The combination of precipitation and solid solution hardening for both alloys FA0.2C and Fe-26Al-2Nb-1C^[17] was supposed. The surprising similarity of $\sigma_{0.2}$ values in spite of the higher f_v of niobium carbides of alloy Fe-26Al-2Nb-1C^[17] is due to the improper size and shape of carbide particles in Reference 17.

Such as the highest values of $\sigma_{0.2}$ of the alloy with only precipitation hardening—FA0.8C with the eutectic net consisting of very fine NbC precipitates—are well understandable.

The results of EBSD and EDX analysis indicate that the strengthening in both investigated alloys is governed by incoherent NbC precipitates. It is obvious that the alloy with higher volume fraction of carbides—FA0.8C ($f_v = 1.7$ pct)—can make the yield stress $\sigma_{0.2}$ in temperature range 473 K to 873 K (200 °C to 600 °C) about 80 MPa higher than the yield stress $\sigma_{0.2}$ of FA0.2C in which only $f_v = 0.6$ pct is available. For the enhancing of the strengthening by the solid solution hardening, only 0.9 at. pct Nb is available in the matrix in the case of alloy FA0.2C, which is obviously not sufficient.

The TEM microstructure investigation of FA0.2C and FA0.8C alloys^[18] shows that fine and scarcely distributed NbC precipitates in FA0.2C alloy have a low

Table I. The Chemical (Present Paper) and Nominal (Ref. [16]) Composition of Investigated Alloys (At. Pct)

Alloy	Fe	Al	Nb	C	$c_{\text{Nb}}/c_{\text{C}}$
FA0.2C	bal	27.6	1.2	0.2	6
FA0.8C	bal	27.1	1.1	0.8	1.4
Fe-26Al-2Nb-1C ^[16]	bal	26	2	1	2

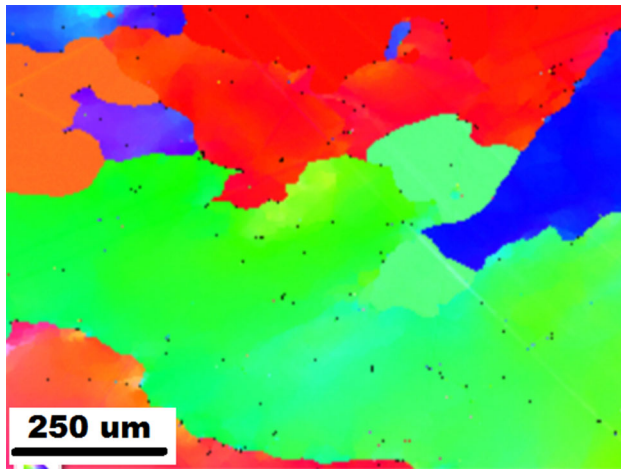


Fig. 1—The grains of FA0.2C alloy (EBSD).

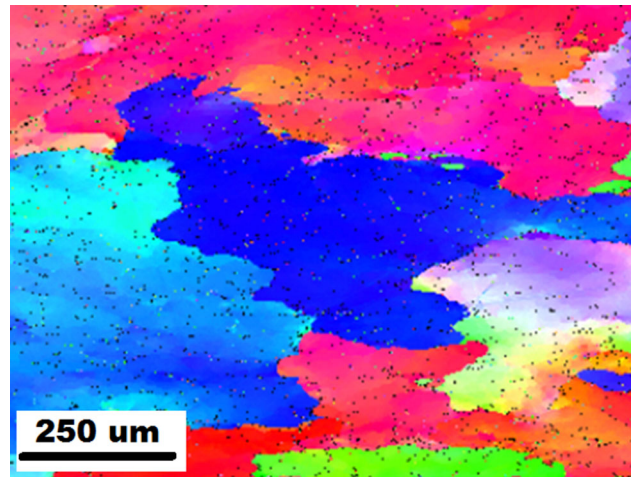


Fig. 4—The grains of FA0.8C alloy (EBSD).

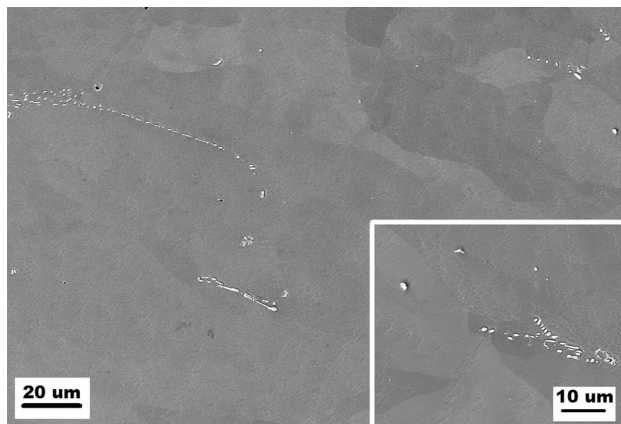


Fig. 2—The structure of FA0.2C alloy; Gray: Fe₃Al matrix, white: NbC particles.

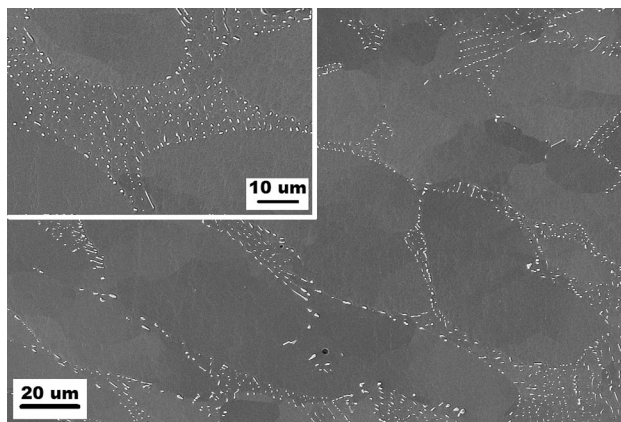


Fig. 3—The structure of FA0.8C alloy; Gray: Fe₃Al matrix, white: NbC particles.

ability to block of dislocation movement. On the other hand, the bigger NbC precipitates in FA0.8C^[18] block of dislocation movement more effectively. This can be the reason for higher values of yield stress for FA0.8C in temperature range from low temperatures to 973 K

Table II. The Volume Fraction (f_v) of NbC and the Nb Concentration in Matrix

Alloy	f_v of NbC (Pct)	Nb in Matrix (At. Pct)
FA0.2C	0.6	0.9
FA0.8C	1.7	—
Fe-26Al-2Nb-1C ^[16]	4.2*	0.6

*Value from the image analysis of picture in Ref. [16].

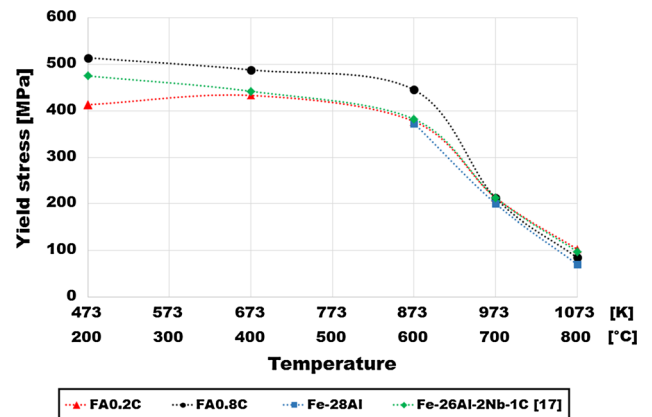


Fig. 5—The comparison of HT yield stress curves for FA0.2C, FA0.8C, Fe-28Al, and Fe-26Al-2Nb-1C.

(700 °C). At HT, the $\sigma_{0.2}$ are the same for both investigated alloys and also for Fe-26Al-2Nb-1C^[17] and binary Fe-28Al. It can be caused by small amount of present strengthening phase (see f_v Table II). Rarely distributed incoherent NbC precipitates are not able to block dislocation movement effectively at HT and the material creeps only in the matrix similarly to binary alloy.

It can be summarized that the main strengthening effect in low Nb and C-alloyed iron aluminides seems to

be strengthening by incoherent precipitates of NbC. From point of view carbon affinity to carbide forming elements, the behavior of iron aluminides doped by Nb is somewhat similar to that doped by Zr.^[19]

IV. CONCLUSIONS

1. The presence of carbon even in small concentrations must be taken in account due to very high affinity of C to the carbide forming element (Nb). The formation of strengthening Laves phase λ_1 (Fe, Al)₂Nb in Fe₃Al iron aluminides alloyed by C is suppressed at the expense of NbC formation.
2. For small Nb concentration or similar Nb and C amount (Nb/C \approx 1), the alloy is reinforced by incoherent NbC precipitates and/or solid solution hardening by surplus niobium. The strengthening effect by higher f_v of NbC precipitates is more beneficial than the combination of strengthening by solid solution hardening and by lower f_v of NbC up to 973 K (700 °C).
3. The values of $\sigma_{0.2}$ are the same for both alloys and also for binary Fe-28Al at HT 973 K to 1073 K (700 °C to 800 °C). It can be caused by low-volume fraction of strengthening phase for effective dislocation movement blocking.

ACKNOWLEDGMENTS

This publication was written at the Technical University of Liberec as part of the project “The study and evaluation of the material’s structure and properties” with the support of the Specific University Research Grant, as provided by the Ministry of Education, Youth and Sports of the Czech Republic in the year 2017. Authors also wish to thank the Centre for nanomaterials, advanced technologies and innovation for realization of EBSD analysis.

LIST OF SYMBOLS

f_v	Volume fraction of precipitates
c_{Nb}	Niobium concentration
c_{C}	Carbon concentration
$\sigma_{0.2}$	Compression yield stress
HT	High-temperature
SEM	Scanning electron microscopy
EDX	Energy-dispersive X-ray analysis
BSE	Backscattered electrons
EBSD	Electron backscatter diffraction

REFERENCES

1. N.S. Stoloff, C.T. Liu, and S.C. Deevi: *Intermetallics*, 2001, vol. 8, pp. 1313–20.
2. A.C. Lilly, S.C. Deevi, and Z.P. Gibbs: *Mater. Sci. Eng.*, 1998, vol. A258, pp. 42–49.
3. M. Palm: *Intermetallics*, 2005, vol. 13, pp. 1286–95.
4. D.G. Morris and M.A. Muñoz-Morris: *Mater. Sci. Eng. A*, 2007, vol. 462, pp. 45–52.
5. C.G. McKamey, P.J. Maziasz, and J.W. Jones: *J. Mater. Res.*, 1992, vol. 7, pp. 2089–2106.
6. C.G. McKamey, P.J. Maziasz, G.M. Goodwin, and T. Zacharia: *Mater. Sci. Eng. A*, 1994, vol. 174, pp. 59–70.
7. C.G. McKamey and P.J. Maziasz: *Intermetallics*, 1998, vol. 6, pp. 303–14.
8. D.G. Morris, M.A. Muñoz-Morris, L.M. Requejo, and C. Baudin: *Intermetallics*, 2006, vol. 13, pp. 1204–07.
9. D.G. Morris, L.M. Requejo, and M.A. Muñoz-Morris: *Scripta Mater.*, 2006, vol. 54, pp. 393–97.
10. D.G. Morris, L.M. Requejo, and M.A. Muñoz-Morris: *Intermetallics*, 2005, vol. 13, pp. 862–71.
11. D.G. Morris and M.A. Muñoz-Morris: *Mater. Sci. Eng. A*, 2012, vol. 552, pp. 134–44.
12. X.Q. Yu and Y.S. Sun: *J. Mater. Sci. Lett.*, 2001, vol. 20, pp. 1221–23.
13. R.G. Baligidad: *J. Mater. Sci.*, 2004, vol. 39, pp. 5599–5602.
14. R.G. Baligidad: *Mater. Sci. Eng.*, 2004, vol. A368, pp. 131–38.
15. S. Milenkovic and M. Palm: *Intermetallics*, 2008, vol. 16, pp. 1212–18.
16. A. Schneider, L. Falat, G. Sauthoff, and G. Frommeyer: *Intermetallics*, 2003, vol. 11, pp. 443–50.
17. L. Falat, A. Schneider, G. Sauthoff, and G. Frommeyer: *Intermetallics*, 2005, vol. 13, pp. 1256–62.
18. F. Dobeš, P. Kratochvíl, J. Pešička, and V. Vodičková: *Mettal. Mater. Trans. A*, 2015, vol. 46A, pp. 1580–87.
19. P. Kratochvíl, V. Vodičková, R. Král, and M. Švec: *Metall. Mater. Trans. A*, 2016, vol. 47A, pp. 1128–32.